The Cell-Free mMIMO Network based on IRSs: Mathematical Analysis and Performance Evaluation

Mohamed Saeid Shalaby (mhmd_shlpy@yahoo.com)
Free Engineer
Mina Wagih Lamie
Faculty of Electronic Engineering
Mona Mohamed Sabry Shokair
Faculty of Electronic Engineering

Research Article

Keywords: mMIMO, Cell-Free networks, IRSs, MRC, SE, and EE

Posted Date: February 4th, 2022

DOI: https://doi.org/10.21203/rs.3.rs-874794/v1

The Cell-Free mMIMO Network based on IRSs: Mathematical Analysis and Performance Evaluation

Mohamed Shalaby (1) , Mina Wagih Lamie (2), and Mona Shokair (2)

(1) Higher Institute of Engineering and Technology in Tanta, Egypt
(2) Faculty of Electronic Engineering, Menoufia University, Menouf, Egypt
Emails: mhmd_shlpy@yahoo.com, minawagih0810@gmail.com, and mona.sabry@el-eng.menofia.edu.eg

Abstract

The massive multiple input multiple output mMIMO technology can improve the cellular system performance especially the cell edge users. Thanks to the large number of implemented antennas at both transmitters and receivers, the mMIMO technology is qualified to satisfy the requirements of the 5G networks and beyond. The Cell-Free network, wherein large spatially distributed antennas are implemented, can improve the performance of shadowed users and indoor ones. In this paper, there is a trial to improve the cell-Free mMIMO network performance by implementation of Intelligent Reflecting Surfaces IRSs. The Cell-Free mMIMO network based on IRSs is mathematically analyzed and simulated. The signals to interference plus noise ratio SINR as well as spectral efficiency SE are derived in closed form formula. It can be concluded that implementation of IRSs in Cell-Free mMIMO networks can increase the SE and EE performance for all cooperation levels.

Key Words: mMIMO, Cell-Free networks, IRSs, MRC, SE, and EE.

1. Introduction

In the 5G networks and beyond, there are a lot of tools that can be applied. These tools can include but not limited to; small cells, multiple input multiple output MIMO, massive MIMO mMIMO, beam forming, and much more. The small size cells can allow cellular systems to reuse the same resources a lot of times. The resource reuse results in a high system capacity. In addition, it can allow low distance communication between a base station and user equipment. Furthermore, application of small size cells is a powerful tool towards high spectral efficiency SE and green communication systems [1-4].

The MIMO techniques can aid a communication system to carry out; beamforming, spatial multiplexing, and diversity gains. The mMIMO, wherein a large number of antennas are applied at a transmitter and a receiver, can provide more beamforming gain and other gains than MIMO systems. Thanks to the high number of implemented antennas at both a transmitter and a receiver, the mMIMO systems can provide more gains in comparable with the MIMO ones. In fact, a mobile cellular system can apply up to 64 antennas at each base station whereas two antennas only can be applied at a mobile station [5-8]. The MIMO and mMIMO can provide large uplink and down link capacities. However, there are a lot of weak points such as; indoor service coverage, cell-edge users, shadowed users, dead zones users, and much more. The users, located at these zones, may have a very low performance.

The Cell-Free mMIMO is a modified version of a mMIMO technology wherein the large number of antennas, which are implemented at a base station, is replaced with distributed APs through the coverage area. For more clarifications, the number of APs in a Cell-Free mMIMO is equal to the same number of antennas at a cellular mMIMO base station. The Cell-Free mMIMO architecture is displayed in Figure 1. There were a lot of researches that handled the mathematical analysis and simulation models for a Cell-Free mMIMO communication system [9]. Four levels of cooperation, among the APs, were considered. In addition, a lot of simulation models in Mathlab exist. As the Cell-Free mMIMO is a powerful tool towards the 5G networks and beyond, a lot of research works were devoted to this topic.

The Cell-Free mMIMO system was mathematically analyzed and there were trials to improve the system performance during application of low resolution analog to digital converters [10]. The authors assumed that there were a lot of APs and users. They provided a novel spectral efficiency SE mathematical equation regarding the quantization noise. They enhanced the SE performance of a Cell-Free mMIMO system. Others tried to improve the uplink system performance by applications of zero-forcing ZF and conjugate beamforming CB [11]. Moreover, the authors provided a tight approximate rate for the ZF receiver. In addition, they considered the impacts of multi-antenna access point AP, estimation error, pilot contamination, and power control schemes.

The operation of small cells and Cell-Free mMIMO is dominated by line of sight LOS propagation. However, the NLOS propagation may exist due to fading effects, mobility, and much more. In Ref. [12], the authors analyzed the Cell-Free mMIMO system assuming correlated fading channels. Moreover, they tried to minimize the downlink consumed power per each antenna in order to reduce the total consumed power in the system as whole. Since the green communication is a necessity towards the 5G networks and beyond, it is necessary to have a power efficient Cell-Free mMIMO system. Therefore, a scalable and energy efficient IOT system, with massive connectivity, was designed in Ref. [13].

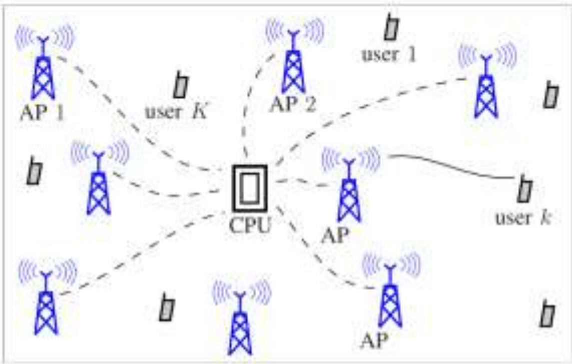

Figure 1: The Cell-Free mMIMO network [9].

One of the powerful techniques towards the 5G networks and beyond is application of the so called non-orthogonal multiple access NOMA technology. NOMA can describe the resource allocation among users in a cellular system. It can allow more resource reuse in power domain. As the resource reuse increases, the system capacity can increase. It is a great idea to have a Cell-Free mMIMO system based on NOMA [14]. The Cell-Free mMIMO, based on NOMA with conjugate beamformer preceding, was analyzed and simulated. The authors held a comparison between NOMA based Cell-Free mMIMO system and OMA one in order to clarify the NOMA advantages. Furthermore, they deduced a novel achievable closed-form SE expression that can characterize the effects of the channel estimation error, pilot contamination, imperfect successive interference cancellation “SIC” operation, and power optimization technique.

The performance metrics of a Cell-Free mMIMO are; SE and EE. Therefore, these metrics should be optimized and improved. The authors of Ref. [15] introduced a novel and comprehensive optimization problem for SE and EE. Their analysis depended on power control mechanisms combined with AP selection. It was a great and a powerful tool to improve the Cell-Free mMIMO performance. The authors of Ref. [16] developed the work of Ref. [10] in order to introduce a mixed analog to digital converter ADC receiver architecture to a Cell-Free mMIMO system under Rician fading channels. The mixed ADC architecture permits some of receiver's antennas to be implemented with economical low resolution ADCs while the rests are equipped with high priced perfect ADCs.

The Cell-Free mMIMO is still under research and a lot of challenges should be solved. The non-orthogonal multiple access NOMA is a powerful tool in Cell-Free mMIMO systems. In Ref. [17], the power domain NOMA techniques were investigated. As mentioned in the previous paragraphs, application of Cell-Free mMIMO with NOMA can provide a high SE and EE communication system. In Ref. [18], the authors carried out an overview and outlook on the architecture, modeling, design, and performance of massively distributed antenna systems DAS with non ideal optical fronthauls. Complex interactions between optical fronthauls and wireless access links require optimum designs across the optical and wireless domains by jointly exploiting their unique characteristics.

The green communication systems can provide a high EE levels. In Ref. [19], the authors designed a power efficient Cell-Free mMIMO network. Their analysis depended on downlink operation only. Subsequently, the SE was maximized in Ref. [20] when two-way half duplex decode and forward DF relaying system with multiple pairs of single antenna users are applied in a Cell-Free mMIMO system. The spatial diversity and coverage are improved. Others proposed adaptation between small cells and Cell-Free mMIMO in order to have a maximum SE performance [21]. Finally, there is a mathematical model for a Cell-Free mMIMO system. This model considered the impact of channel aging on the uplink performance of a Cell-Free mMIMO system with a minimum mean squared error MMSE receiver [22].

The Cell-Free mMIMO network was mathematically modeled and simulated [23]. The Cell-Free mMIMO network can operate by applying four levels of cooperation mechanisms. The simulation was carried out through application of different number of APs and different number of antennas per each AP. Moreover, the SE of different users as well as the sum of spectral efficiency, after applying interference cancellation mechanisms, was simulated. Furthermore, in the previously mentioned work, the SE and EE, based bit error rate BER, performance of a Cell-Free mMIMO system were mathematically analyzed in a closed form formula.

Intelligent reflecting surfaces IRSs are competing techniques to relays. However, IRSs can aid in signal improvement to receivers without noise amplification. IRSs can enable a receiver to have gains from multiple reflections. These reflections can enhance each other. The IRSs can be used in order to focus energy in a direction. In addition, they may be used in order to cancel out signal "prevent" in a direction. In other word, IRSs can be applied as ubiquitous directive antennas. The best position to implement an IRs is to be at the transmitter or a receiver.

In this paper, the IRSs are implemented in a Cell-Free mMIMO system in order to let each AP deliver their information signal to users with little power. The receiver can combine both received signal coming from original transmitters as well as that are reflected from IRSs. Therefore, the received power is enhanced. When the received signal is improved, the signal to noise ratio is enhanced. As a result, the SE will be improved. In other words, combination of the transmitter signals and their IRS reflected versions can let the original transmitter send with low power. In conclusion, it is predicted that the Cell-Free mMIMO systems, based on IRSs, have a high SE and EE performance especially when the MRC is applied.

Our paper is organized as follows; Section 2 provides the mathematical analysis of the Cell-Free mMIMO network that is based on IRSs. Subsequently, the proposed system is simulated and performance comparisons are held in Section 3. Finally, conclusions are given in Section 4.

2. IRSs Based Cell-Free mMIMO System

Consider a cell-Free mMIMO network model that has L distributed APs. Each AP has N antennas. The APs are connected over a centralized controller "cloud-edge processor". These APs can serve K users. Assume that $h_{k,l}$ describes the channel between l AP and the k user. The coefficients of the channel vectors are assumed to have Rayleigh distribution. The relays are randomly distributed inside the coverage area.

The cell-Free mMIMO system is implemented assuming that the operation is in uplink. The UEs are transmitters whereas the APs are receivers. The APs can receive each data segment from UEs as well as relays. A relay can receive the UE signal and then, forward it to an AP. In fact, there are a lot of relaying strategies. However, this paper considers a traditional relay that follows decode and forward strategy.

2.1. Pilot Transmission

Assume that there are mutually orthogonal pilot signals which are; $\varphi_1, \varphi_2, \varphi_3, \ldots, \varphi_{\tau p}$. These pilots are used for channel estimation during data transmission period. Since the pilots are used for control processes only, the total pilot length should not exceed 20% of total frame time in order to save the data rate.

The total available pilots can be divided into two group and they are;

- Group 1 is a summation of pilots that are applied to estimate the channel between UEs and IRSs.
- Group 2 is a summation of pilots that are applied to estimate the channel between UEs and APs.

The total pilot length is τ_p. The total pilot length is divided into two equal parts. Each part has a length of $\tau_p /2$. Due to the limited number of pilots, the number of users may be higher than the number of pilots. A lot of users can operate on a pilot which results in a pilot contamination. In the proposed work, the pilots are divided into two groups. This division results in increased pilot contamination [23]. When the UEs transmit their pilots, the received pilot at an IRS can be expressed as;

$$\boldsymbol{Z}_{lSR} = \sum_{i=1}^{k} \sqrt{p_i}\, \boldsymbol{\beta}_{SRil} \emptyset_{t_i}^{T} + \boldsymbol{N}_{LSR} \qquad\qquad 0 \le t \le \frac{\mathcal{T}_p}{2} \tag{1}$$

The pilots, that are applied to estimate the channel between a UE and an AP, can be mathematically expressed as;

$$\boldsymbol{Z}_{lSD} = \sum_{i=1}^{k} \sqrt{p_i}\, \boldsymbol{\beta}_{SDil} \emptyset_{t_i}^{T} + \boldsymbol{N}_{LSD} \qquad\qquad \frac{\mathcal{T}_p}{2} + 1 \le t \le \mathcal{T}_p \tag{2}$$

where $\mathbf{p}_i$ is the transmit power of i^{th} user, $\boldsymbol{\beta}_{SR}$ is the channel vector between a UE and an IRS, $\boldsymbol{\beta}_{SD}$ is the channel vector between a UE and an AP. The parameter of $\mathbf{N}_{LSR}$ and $\mathbf{N}_{LSD}$ is the noise signals. To estimate the channel parameters, each AP should correlate the received pilot signals with a locally generated version of the pilot signal in order to determine the channel parameters.

The received pilot signal at an IRS is that comes from UEs. This pilot can be applied in order to estimate the wireless channel between a UE and an IRS. The received pilot is correlated with a locally generated replica. This correlation can be mathematically expressed as follow;

$$Z_{t_k l} = \sum_{i=1}^{k} \frac{\sqrt{p_i}}{\sqrt{\frac{\mathcal{T}_p}{2}}} \boldsymbol{\beta}_{SRil}\, \emptyset_{t_i}^{T}\ \emptyset_{t_k}^{*} + \frac{1}{\sqrt{\frac{\mathcal{T}_p}{2}}} \boldsymbol{N}_{LSR} \emptyset_{t_k}^{*} = \sum_{i \in P_k} \sqrt{\frac{p_i \mathcal{T}_p}{2}}\ \boldsymbol{\beta}_{SRil} + \boldsymbol{n}_{t_k l} \tag{3}$$

where $\frac{\mathcal{T}_p}{2}$ is the time allowed for pilot transmission. By using the *MMSE* to estimate the channel parameter between a UE and an IRS, $\hat{\beta}_{SRkl}$, can be given by;

$$\hat{\beta}_{SRkl} = \sqrt{\frac{p_k \mathcal{T}_p}{3}} \boldsymbol{R}_{kl}\, \Psi_{t_k l}^{-1}\, z_{t_k l} \tag{4}$$

where;

$$\Psi_{t_k l} \ = \ \mathbb{E}\left\{ \boldsymbol{z}_{t_k l}\, \boldsymbol{z}_{t_k l}^{H} \right\} = \sum_{i \in P_k} \frac{\mathcal{T}_p}{3}\ p_i \boldsymbol{R}_{il}\ + \boldsymbol{I}_N \tag{5}$$

Eq. 5 gives an expression for the correlation matrix of the received pilot signal at an IRS.

The received pilot signal at an AP is that comes from UEs. This plot can be applied in order to estimate the wireless channel between a UE and an AP. The received pilot is correlated with a locally generated replica. This correlation can be mathematically expressed as follow;

$$Z_{t_k l} = \sum_{i=1}^{k} \frac{\sqrt{p_i}}{\sqrt{\frac{\mathcal{T}_p}{2}}} \boldsymbol{\beta}_{SDil}\, \emptyset_{t_i}^{T}\ \emptyset_{t_k}^{*} + \frac{1}{\sqrt{\frac{\mathcal{T}_p}{2}}} \boldsymbol{N}_{LSD} \emptyset_{t_k}^{*} = \sum_{i \in P_k} \sqrt{\frac{p_i \mathcal{T}_p}{2}}\ \boldsymbol{\beta}_{SDil} + \boldsymbol{n}_{t_k l} \tag{6}$$

where $\frac{\mathcal{T}_p}{2}$ is the time allowed for pilot transmission By using the *MMSE* to estimate the channel parameter between a UE and an AP, $\hat{\beta}_{SDkl}$, can be given by;

$$\hat{\beta}_{SDkl} = \sqrt{\frac{p_k \mathcal{T}_p}{2}} \boldsymbol{R}_{kl}\, \Psi_{t_k l}^{-1}\, z_{t_k l} \tag{7}$$

where;

$$\Psi_{t_k l} \ = \ \mathbb{E}\left\{ \boldsymbol{z}_{t_k l}\, \boldsymbol{z}_{t_k l}^{H} \right\} = \sum_{i \in P_k} \frac{\mathcal{T}_p}{3}\ p_i \boldsymbol{R}_{il}\ + \boldsymbol{I}_N \tag{8}$$

Eq. 8 gives an expression for the correlation matrix of the second received pilot signal at an AP.

2.2. Data Transmission

During the uplink data transmission, the total received complex base band signals at an AP “coming from both a UE and an IRS” can be mathematically modeled as;

$$y = \sum_{i=1}^{k} \boldsymbol{\beta}_{SDil}\ s_i + \sum_{i=1}^{k} \boldsymbol{\beta}_{RDil}\ s_R + n \tag{9}$$

where y is the received signal, $\boldsymbol{S}_i$ is the transmitted signal from a UE, while $\boldsymbol{S}_R$ is the IRS transmitted signal, n is the channel noise, and $\boldsymbol{\beta}_{RD}$ is the channel vector between an IRS and an AP, $\boldsymbol{\beta}_{SD}$ is the channel vector between a UE and an AP that can include the path loss as well as shadowing.

2.2.1 Cooperation among the APs

The basic concept depends on the idea of the Cell-Free mMIMO network based on IRSs. The coverage area is totally covered by distributed APs, in such a way that, user equipment can have a service from the nearest AP as well as the nearest IRS. Combination between AP signal and the IRS one can improve the received SNR. Moreover, it can let the system be a power efficient one. The cooperation among the several APs and relays can be carried out by four levels which are stated below.

- **Fully Centralized APs "Level 4"**

During this cooperation mechanism, both APs and IRSs can provide service for the users in downlink. On the other side, during uplink, the APs can receive the signals from UEs as well as IRSs. Therefore, the received signal is enhanced at each AP. Really each AP can forward pilots and data to a central controller where the processing can be carried out. The centralized controller can have processing capability more than an AP. The received signal, Y, can be expressed as discussed in Eq. 9.

The signal to interference plus noise ratio, *SINR*, and the spectral efficiency, *SE*, and can be calculated by the following relations;

$$SINR_k^{(4)} = \frac{p_k\left|V_k^H\,\hat{\beta}_{SDK}\right|^2 + p_k\left|V_k^H\,\hat{\beta}_{RD}\right|^2}{\sum_{i=1,i\neq k}^{k} p_i |V_k^H\,\beta_{SDi}|^2 + V_k^H\left(\sum_{i=1}^{k} p_i\,\boldsymbol{C}_i + \boldsymbol{\sigma^2 I_{LN}}\right) V_k} \tag{10}$$

$$SE_K^{(4)} = \frac{1}{2}\left(\ 1-\frac{\mathcal{T}_p}{\mathcal{T}_c}\ \right)\mathbb{E}\left\{\ log_2\left(1+\beta_{SD}\,SINR^{(4)} + \beta_{SR}\beta_{RD}\times\ SINR^{(4)}\right)\ \right\} \tag{11}$$

With the help of Ref. [23], the energy efficiency, *EE*, can be expressed as;

$$EE = BW\frac{SE}{P_c + P_T} \tag{12}$$

where *BW* is the bandwidth, P_C is the power consumed in the circuits, and P_T is the transmitted power. The transmission power, during the uplink is the mobile equipment power as well as relays. The *EE* may be calculated per unity *BW* value.

- **Level 3**

During this level of cooperation, APs can receive from UEs and IRSs. Each AP can detect pilots in order to perform channel estimation. Then, the estimated channel parameters associated with the received data signals are sent to a centralized controller. This controller can detect the data signal based on the given channel estimates. This level can largely simplify the complexity of computation at the central controller. The signal to interference plus noise ratio, *SINR*, and the *SE* can be expressed as;

$$SINR_k^{(3)} = \frac{p_k\left|a_k^H\mathbb{E}\left\{g_{kk}\right\}\right|^2\Big|S+p_k\left|a_k^H\mathbb{E}\left\{g_{kk}\right\}\right|^2\Big|R}{\sum_{i=1}^{k} p_i\,\mathbb{E}\left\{\left|a_k^H g_{ki}\right|^2\right\}\Big|S+R-p_k\left|a_k^H\mathbb{E}\left\{g_{kk}\right\}\right|^2\Big|S+R+\sigma^2 a_k^H \mathrm{D}_k a_k} \tag{13}$$

$$SE_K^{(3)} = \frac{1}{2}\left(\ 1-\frac{\mathcal{T}_p}{\mathcal{T}_c}\ \right) log_2\left(1+\boldsymbol{\beta}_{SD}SINR_k^{(3)} + \beta_{SR}\beta_{RD}\times\ SINR_k^{(3)}\ \right) \tag{14}$$

- **Level 2**

During this level of cooperation, APs can receive from UEs and IRSs. The centralized controller can receive the estimated channel parameters and the received data. Then, it can detect the received data based on the average of the channel estimates. Averaging the channel estimates can simplify the computation complexity that is required at a centralized controller. The spectral efficiency, *SE*, and the signal to interference plus noise ratio, *SINR*, can be calculated by the following relations;

$$SE_K^{(2)} = \frac{1}{2}\left(\ 1-\frac{\mathcal{T}_p}{\mathcal{T}_c}\ \right) log_2\left(1+\boldsymbol{\beta}_{SD}SINR_k^{(2)} + \beta_{SR}\beta_{RD}\times SINR_k^{(2)}\right) \tag{15}$$

$$SINR_k^{(2)} = \frac{p_k\left|\sum_{i=1}^{k}\mathbb{E}\left\{V_{kl}^H\boldsymbol{\beta}_{SDl}\right\}\right|^2 + p_k\left|\sum_{i=1}^{k}\mathbb{E}\left\{V_{kl}^H\boldsymbol{\beta}_{RDl}\right\}\right|^2}{\sum_{i=1}^{k} p_i\,\mathbb{E}\left\{\left|\sum_{l=1}^{L} V_{kl}^H\boldsymbol{\beta}_{SDil}\right|^2\right\}\Big|S+R-p_k\left|\sum_{l=1}^{k}\mathbb{E}\left\{V_{kl}^H\boldsymbol{\beta}_{SDkl}\right\}\right|^2\Big|S+R+\sigma^2\sum_{l=1}^{k}\mathbb{E}\left\{\|V_{kl}\|^2\right\}} \tag{16}$$

The energy efficiency, *EE*, can be calculated by applying a unity *BW* value in Eq. 16.

- **Fully Distributed Level 1**

During this level of cooperation, APs can receive from UEs and IRSs. The *APs* can detect both pilot signal and data signal. The processing functions are carried out at the *APs*. Therefore, the centralized controller is free from pilot or data detection. The centralized controller, in this case, can provide cooperation among the *APs* only when it receives the detected pilots and estimated data for all users. The spectral efficiency, *SE*, and the signal to interference plus noise ratio, *SINR*, can be calculated by the following relations;

$$SE_K^{(1)} = \frac{1}{2}\left(1 - \frac{\mathcal{T}_p}{\mathcal{T}_c}\right) \max_{l \in \{1,\ldots,L\}} \mathbb{E}\left\{ log_2\left(1 + \boldsymbol{\beta}_{SD} SINR_k^{(1)} + \beta_{SR}\beta_{RD} \times SINR_k^{(1)}\right)\right\} \tag{17}$$

$$SINR_{kl}^{(1)} = \frac{p_k \left|V_{kl}^H \widehat{\boldsymbol{\beta}}_{SDKl}\right|^2 + p_k \left|V_{kl}^H \widehat{\boldsymbol{\beta}}_{RDKl}\right|^2}{\sum_{\substack{i=1,\\ i \neq k}}^{k} p_i \left|V_{kl}^H \boldsymbol{\beta}_{SDil}\right|^2 + V_{kl}^H\left(\sum_{i=1}^{k} p_i \,\boldsymbol{C}_{il} + \boldsymbol{\sigma}^2 \boldsymbol{I}_N\right) V_{kl}} \tag{18}$$

The *EE* can be calculated as in Eq. 12.

3. Simulation Results

In this section, the Cell-Free network based on IRSs is simulated. The simulation parameters are concluded in Table 1. The cell radius is 20 m. In addition, the IRSs are randomly distributed inside the coverage area. However, the best place of an IRS deployment is at the UE or at AP. The channel propagation and fading models are applied according to 3GPP standard [23]. The path loss models are given in Eq. 19 and Eq. 20. These models are applied in fore-mentioned work [23].

$$\beta_{kl}[dB] = -30.5 - 36.7\, log_{10}\left(\frac{d_{kl}}{1m}\right) + F_{kl} \tag{19}$$

$$\mathbb{E}\left\{F_{kl}\, F_{ij}\right\} = \begin{cases} 4^2 2^{-\delta_{ki}/9m} & l = j \\ 0 & l \neq j \end{cases} \tag{20}$$

Figure 2 shows the SE performance of a cell-Free mMIMO system based on IRSs when the MRC is applied. It can be observed that the IRS deployment can enhance the SE performance of a cell-Free mMIMO network. The four levels of cooperation can have a better performance when the IRS exists.

Figure 3 shows the EE performance of a cell-Free mMIMO system based on IRSs when the MRC is applied. It can be observed that the IRS deployment can enhance the EE performance of a cell-Free mMIMO network. The four levels of cooperation can have a better performance when the IRSs exist.

From Figure 2 and Figure 3, it can be observed that the IRS deployment can enhance the SE and EE performance of a cell-Free mMIMO especially for low level users. The low level users may be users at cell edges, shadowed users, and others. Without IRSs, some users may have a zero SE and EE performance. Thanks to the IRS deployment, the users, inside a coverage area, can have a satisfied performance.

Table 1. The simulation parameters.

Parameter		Value
Number of cellular base stations		4
Number of antennas per each base station		100
Area		1×1 km
Fading		Rayleigh Fading
Shadowing	Standard Deviation	4 dB
	Correlation Distance among UEs	0.5 m
	Decorrelation distance	9 m
Noise Figure		9 dB
Bandwidth		20 MHz
Antenna Spacing		0.5
UE Transmission power		20 dBm
Number of UEs		40
P_T		100 mWatt
P_C		0.1 Watt

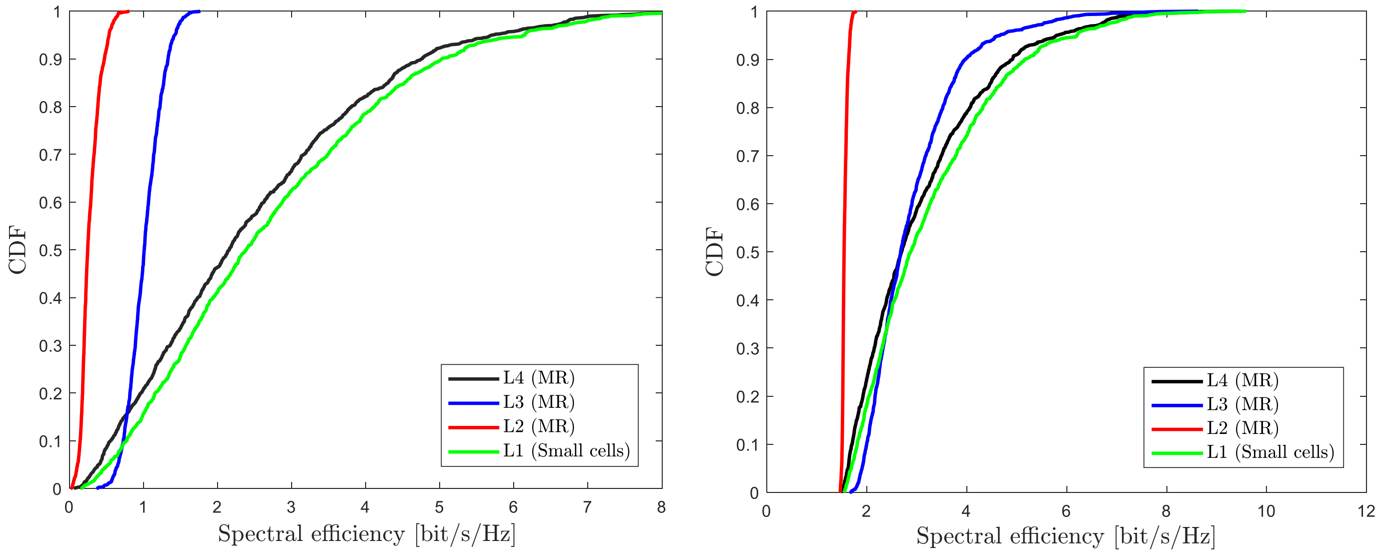

(a) Without IRSs (b) With IRSs

Figure 2: The spectral efficiency performance of a Cell-Free mMIMO system based on IRSs.

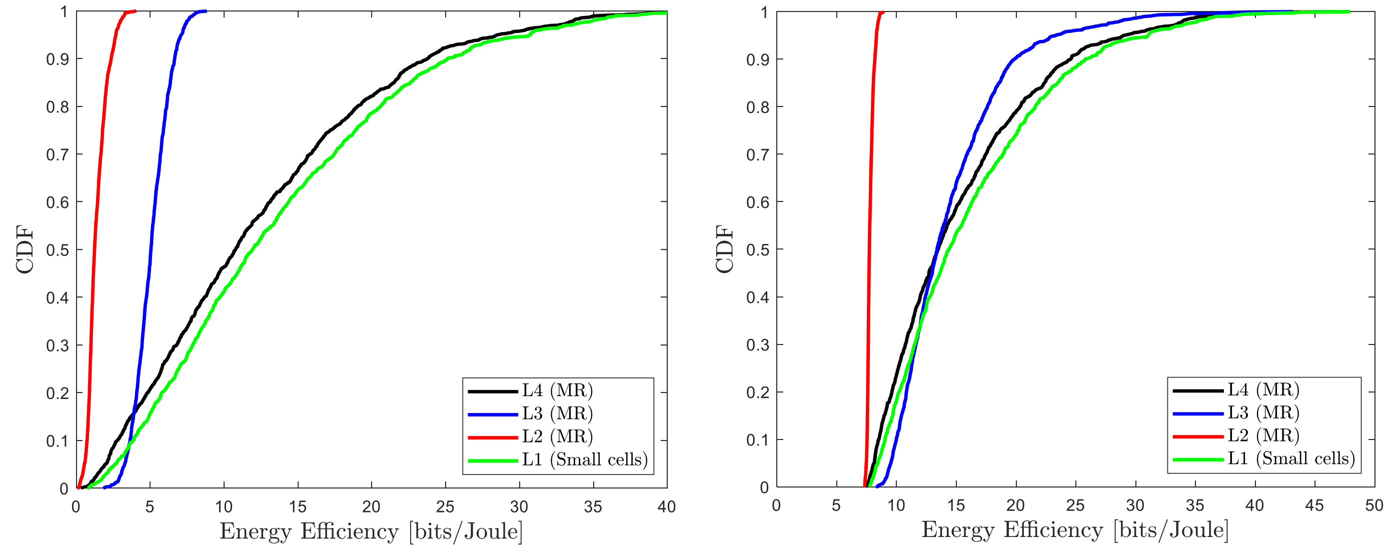

(a) Without IRSs (b) With IRSs

Figure 3: The energy efficiency performance of a Cell-Free mMIMO system based on IRSs.

4. Conclusions

The IRSs are deployed in a cell-Free mMIMO system in order to enhance the performance. Then, the cell-Free mMIMO network, based on IRSs, was mathematically analyzed and simulated. The SE and EE are mathematically analyzed in a closed form formula. It was observed that, the IRS deployment inside a cell-Free mMIMO system can enhance the SE and EE performance for all users even they are shadowed or cell-edge ones.

Declarations

The datasets generated during and/or analyzed during the current study are available from the corresponding author on reasonable request.

Funding source of this work is supported by the faculty of Electronic Engineering, Menoufia University, Menouf, Egypt.

There is no conflict between this work and other published work.

The Mathlab code is available on reasonable request.

References

1. D. Muirhead, M. A. Imran and K. Arshad, "A Survey of the Challenges, Opportunities and Use of Multiple Antennas in Current and Future 5G Small Cell Base Stations," in IEEE Access, vol. 4, pp. 2952-2964, 2016, doi: 10.1109/ACCESS.2016.2569483.
2. Y. Yang, B. Bai and W. Chen, "Spectrum Reuse Ratio in 5G Cellular Networks: A Matrix Graph Approach," in IEEE Transactions on Mobile Computing, vol. 16, no. 12, pp. 3541-3553, 1 Dec. 2017, doi: 10.1109/TMC.2017.2696005.
3. A. Taufique, M. Jaber, A. Imran, Z. Dawy and E. Yacoub, "Planning Wireless Cellular Networks of Future: Outlook, Challenges and Opportunities," in IEEE Access, vol. 5, pp. 4821-4845, 2017, doi: 10.1109/ACCESS.2017.2680318.
4. F. Song et al., "Probabilistic Caching for Small-Cell Networks With Terrestrial and Aerial Users," in IEEE Transactions on Vehicular Technology, vol. 68, no. 9, pp. 9162-9177, Sept. 2019, doi: 10.1109/TVT.2019.2929839.
5. Y. Xin, D. Wang, J. Li, H. Zhu, J. Wang and X. You, "Area Spectral Efficiency and Area Energy Efficiency of Massive MIMO Cellular Systems," in IEEE Transactions on Vehicular Technology, vol. 65, no. 5, pp. 3243-3254, May 2016, doi: 10.1109/TVT.2015.2436896.
6. Shojaeifard, K. Wong, M. Di Renzo, G. Zheng, K. A. Hamdi and J. Tang, "Massive MIMO-Enabled Full-Duplex Cellular Networks," in IEEE Transactions on Communications, vol. 65, no. 11, pp. 4734-4750, Nov. 2017, doi: 10.1109/TCOMM.2017.2731768.
7. Y. Han, B. D. Rao and J. Lee, "Massive Uncoordinated Access With Massive MIMO: A Dictionary Learning Approach," in IEEE Transactions on Wireless Communications, vol. 19, no. 2, pp. 1320-1332, Feb. 2020, doi: 10.1109/TWC.2019.2952843.
8. L. You et al., "Pilot Reuse for Vehicle-to-Vehicle Underlay Massive MIMO Transmission," in IEEE Transactions on Vehicular Technology, vol. 69, no. 5, pp. 5693-5697, May 2020, doi: 10.1109/TVT.2020.2982013.
9. E. Björnson and L. Sanguinetti, "Making Cell-Free Massive MIMO Competitive With MMSE Processing and Centralized Implementation," in IEEE Transactions on Wireless Communications, vol. 19, no. 1, pp. 77-90, Jan. 2020, doi: 10.1109/TWC.2019.2941478.
10. Y. Zhang, M. Zhou, X. Qiao, H. Cao and L. Yang, "On the Performance of Cell-Free Massive MIMO With Low-Resolution ADCs," in *IEEE Access*, vol. 7, pp. 117968-117977, 2019, doi: 10.1109/ACCESS.2019.2937094.
11. Y. Zhang, H. Cao, M. Zhou and L. Yang, "Cell-free massive MIMO: Zero forcing and conjugate beamforming receivers," in *Journal of Communications and Networks*, vol. 21, no. 6, pp. 529-538, Dec. 2019, doi: 10.1109/JCN.2019.000053.
12. J. Qiu, K. Xu, X. Xia, Z. Shen and W. Xie, "Downlink Power Optimization for Cell-Free Massive MIMO Over Spatially Correlated Rayleigh Fading Channels," in *IEEE Access*, vol. 8, pp. 56214-56227, 2020, doi: 10.1109/ACCESS.2020.2981967.
13. S. Chen, J. Zhang, Y. Jin and B. Ai, "Wireless powered IoE for 6G: Massive access meets scalable cell-free massive MIMO," in *China Communications*, vol. 17, no. 12, pp. 92-109, Dec. 2020, doi: 10.23919/JCC.2020.12.007.
14. Y. Zhang, H. Cao, M. Zhou and L. Yang, "Non-orthogonal multiple access in cell-free massive MIMO networks," in *China Communications*, vol. 17, no. 8, pp. 81-94, Aug. 2020, doi: 10.23919/JCC.2020.08.007.
15. H. V. Nguyen *et al*., "On the Spectral and Energy Efficiencies of Full-Duplex Cell-Free Massive MIMO," in *IEEE Journal on Selected Areas in Communications*, vol. 38, no. 8, pp. 1698-1718, Aug. 2020, doi: 10.1109/JSAC.2020.3000810.
16. Y. Zhang, M. Zhou, H. Cao, L. Yang and H. Zhu, "On the Performance of Cell-Free Massive MIMO With Mixed-ADC Under Rician Fading Channels," in *IEEE Communications Letters*, vol. 24, no. 1, pp. 43-47, Jan. 2020, doi: 10.1109/LCOMM.2019.2947462.
17. O. Maraqa, A. S. Rajasekaran, S. Al-Ahmadi, H. Yanikomeroglu and S. M. Sait, "A Survey of Rate-Optimal Power Domain NOMA With Enabling Technologies of Future Wireless Networks," in *IEEE Communications Surveys & Tutorials*, vol. 22, no. 4, pp. 2192-2235, Fourthquarter 2020, doi: 10.1109/COMST.2020.3013514.
18. L. Yu, J. Wu, A. Zhou, E. G. Larsson and P. Fan, "Massively Distributed Antenna Systems With Nonideal Optical Fiber Fronthauls: A Promising Technology for 6G Wireless Communication Systems," in *IEEE Vehicular Technology Magazine*, vol. 15, no. 4, pp. 43-51, Dec. 2020, doi: 10.1109/MVT.2020.3018100.
19. A. Papazafeiropoulos, H. Q. Ngo, P. Kourtessis, S. Chatzinotas and J. M. Senior, "Towards Optimal Energy Efficiency in Cell-Free Massive MIMO Systems," in *IEEE Transactions on Green Communications and Networking*, vol. 5, no. 2, pp. 816-831, June 2021, doi: 10.1109/TGCN.2021.3059206.
20. A. K. Papazafeiropoulos, P. Kourtessis, S. Chatzinotas and J. M. Senior, "Multipair Two-Way DF Relaying With Cell-Free Massive MIMO," in *IEEE Open Journal of the Communications Society*, vol. 2, pp. 423-438, 2021, doi: 10.1109/OJCOMS.2021.3060661.
21. S. Elhoushy and W. Hamouda, "Towards High Data Rates in Dynamic Environments Using Hybrid Cell-Free Massive MIMO/Small-Cell System," in *IEEE Wireless Communications Letters*, vol. 10, no. 2, pp. 201-205, Feb. 2021, doi: 10.1109/LWC.2020.3021026.
22. R. Chopra, C. R. Murthy and A. K. Papazafeiropoulos, "Uplink Performance Analysis of Cell-Free mMIMO Systems Under Channel Aging," in *IEEE Communications Letters*, vol. 25, no. 7, pp. 2206-2210, July 2021, doi: 10.1109/LCOMM.2021.3073778.
23. M. Shalaby, H. M. Hussein, and M. Shokair, “The cell-free mMIMO networks: mathematical analysis and performance evaluation,” Telecommunication Systems, Springer, 77, 625–641 (2021). Available on this link: https://doi.org/10.1007/s11235-021-00776-z.